J. Chem. Sci., Vol. 122, No. 6, November 2010, pp. 901–909.

Theoretical study of nucleophilic halogenalkylation of propylene oxide with halogenmethane and dihalogenmethane anion

TAO LIU[a], XIANG-CHEN YIN[a], GUO-DONG LIU[a] and ZHANG-YU YU[b,c,d,*]

[a]Department of Chemistry and Chemical Engineering, Jining University, Qufu 273155, Shandong, People's Republic of China

[b]School of Chemistry and Chemical Engineering, Shandong University, Jinan 250010, Shandong, People's Republic of China

[c]School of Chemistry and Chemical Engineering, Qufu Normal University, Qufu 273165, Shandong, People's Republic of China

[d]Department of Chemistry and Chemical Engineering, Heze University, Heze 274015, Shandong, People's Republic of China

e-mail: zhy_yu@126.com

MS received 19 October 2009; revised 30 June 2010; accepted 2 September 2010

Abstract. The nucleophilic halogenalkylation reactions of propylene oxide with halogenmethane anion (CH_2X^-) and dihalogenmethane anion (CHX_2^-) (X = F, Cl) in the gas phase and in the Et_2O solvent are studied using the B3LYP method and the SCIPCM model for simulating solution effects. Our calculations predict the same reaction path for following reactions: (1) (X = F, Cl) and (2) (X = F) in the two phases, but there is a little difference in the relative energy of IM1(2Cl) in the gas phase and in the Et_2O solvent for reaction (2) (X = Cl). All the four reactions proceed in two steps. Reactions (1) and (2) are predicted to be exothermic and thermodynamically favourable in both the gas phase and the Et_2O solvent. The overall barrier energies for reaction (1) (X = F), reaction (1) (X = Cl), reaction (2) (X = F), and reaction (2) (X = Cl) are predicted to be 2·74 and 4·08 kcal mol^{-1}, 3·35 and 5·20 kcal mol^{-1}, 4·67 and 6·05 kcal mol^{-1}, and 5·33 and 8·23 kcal mol^{-1} in the gas phase and in the Et_2O solvent, respectively. The accurate calculation of results for the model systems would be useful for experimental researchers working in this field.

Keywords. Nucleophilic halogenalkylation; CH_2F^-; CH_2Cl^-; CHF_2^-; $CHCl_2^-$; propylene oxide.

1. Introduction

Recently, selective incorporation of fluorine atom(s) into organic molecules, commonly called fluoroalkylation, has been widely employed and used as powerful strategy in drug design and materials research.[1,2]

Nucleophilic fluoroalkylation, typically involving the transfer of a fluorine-bearing carbanion to an electrophile, has been widely studied and applied to synthesize fluorine-containing materials and bioactive molecules.[3–15] Despite the availability of a variety of good methods and numerous examples of nucleophilic fluoroalkylation of various substrates,[4–8] there are only a few examples in the literature related to nucleophilic fluoroalkylation of simple epoxides. The possible reason, as stated in the literature,[3] can be attributed to the intrinsic property of the fluorine-bearing carbanion, as well as its weak nucleophilicity toward epoxides. Epoxides play an important role in organic synthesis, in part because the nature of their structure and reactivity allows regio- and stereo-specific carbon-carbon bond formation simultaneous with formation of an adjacent alcohol function.[16]

The study on exploring the ring-opening reaction of epoxides from various sources of carbanion can be fully employed in drug design, organic synthesis and other fields. The purpose of our theoretical work is to investigate the ring-opening mechanisms of epoxides from some sources of carbanion, such as fluoromethane anion (CH_2F^-), difluoromethane anion (CHF_2^-), trifluoromethane anion (CF_3^-), (benzenesulfonyl)monofluoromethane anion ($PhSO_2CHF^-$),[3] and (benzenesulfonyl)difluoromethane anion ($PhSO_2CF_2^-$)[3], and to discuss some useful

*For correspondence

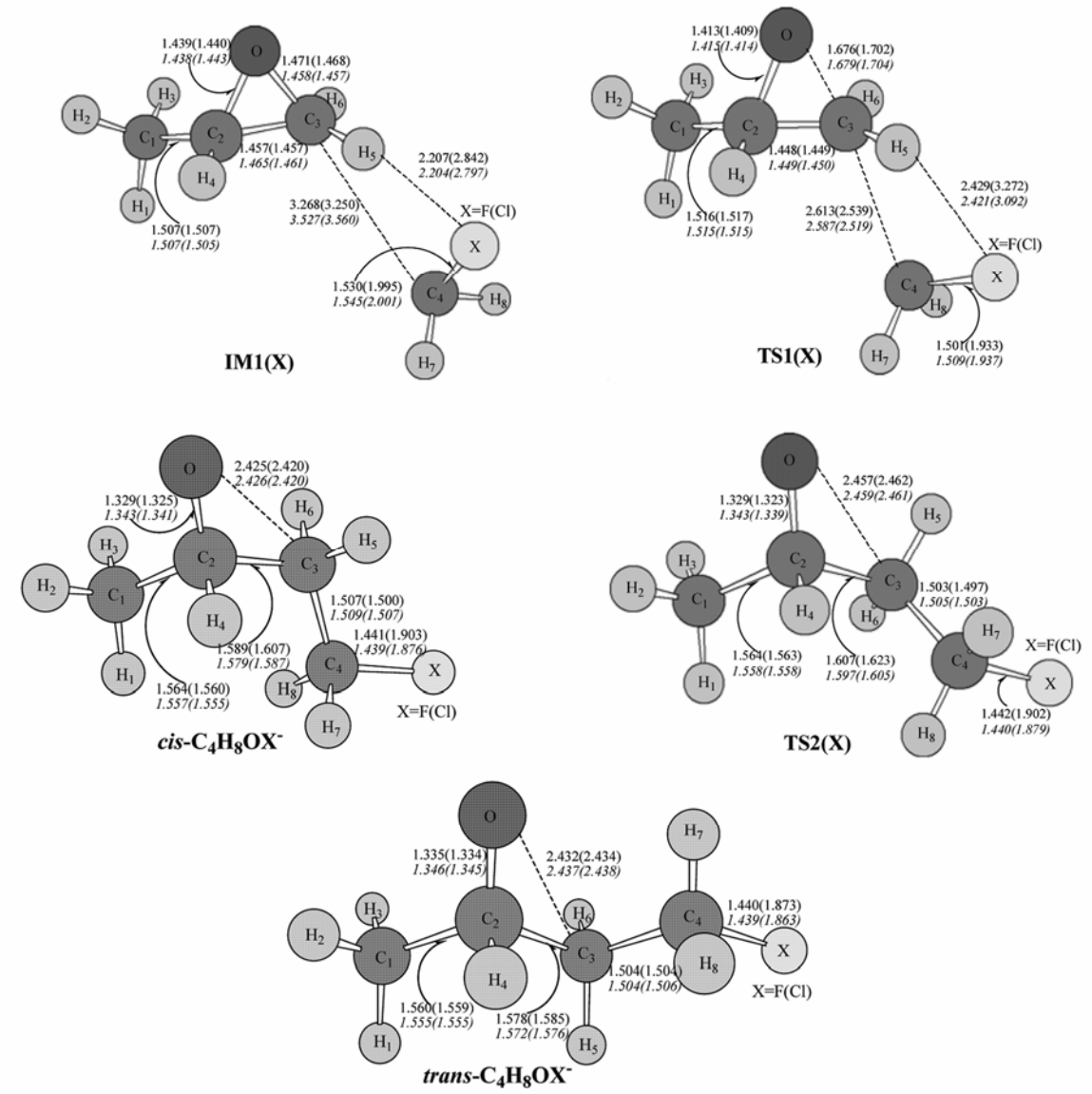

Figure 1. Optimized structures of the intermediate complexes (IM(X)), transition states (TSn(X)), and products (*cis*-$C_4H_8OX^-$ and *trans*-$C_4H_8OX^-$) along the B3LYP/6-311+G** reaction paths in the gas phase and in the Et_2O solvent. Values are the bond distances in Å. The values in italic are the bond distances in the Et_2O solvent and the values in parentheses are the bond distances when X denotes Cl.

results for nucleophilic fluoroalkylation reaction. In the present work, we report the results on the nucleophilic fluoroalkylation of epoxides with CH_2F^- and CHF_2^-, and the results on the reaction of epoxides with CF_3^-, $PhSO_2CHF^-$, and $PhSO_2CF_2^-$ when we find comparable experimental results same would be published.

In the present study, we investigated the nucleophilic fluoroalkylation of propylene oxide, as a model molecule of epoxides, with fluoromethane anion (CH_2F^-) and difluoromethane anion (CHF_2^-). For comparing, we also studied the nucleophilic chloroalkylation of propylene oxide with chloromethane anion (CH_2Cl^-) and dichloromethane anion ($CHCl_2^-$). The following four reaction of propylene oxide with CH_2X^- and CHX_2^- (X = F, Cl) were considered:

$$C_3H_6O + CH_2X^- \rightarrow \textit{cis}\text{-}C_4H_8OX^- \rightarrow \textit{trans}\text{-}C_4H_8OX^- \ (X = F, Cl), \quad (1)$$

$$C_3H_6O + CHX_2^- \rightarrow \textit{cis}\text{-}C_4H_7OX_2^- \rightarrow \textit{trans}\text{-}C_4H_7OX_2^- \ (X = F, Cl), \quad (2)$$

where *cis*-$C_4H_8OX^-$ (*cis*-$C_4H_7OX_2^-$) and *trans*-$C_4H_8OX^-$ (*trans*-$C_4H_7OX_2^-$) are used to represent the

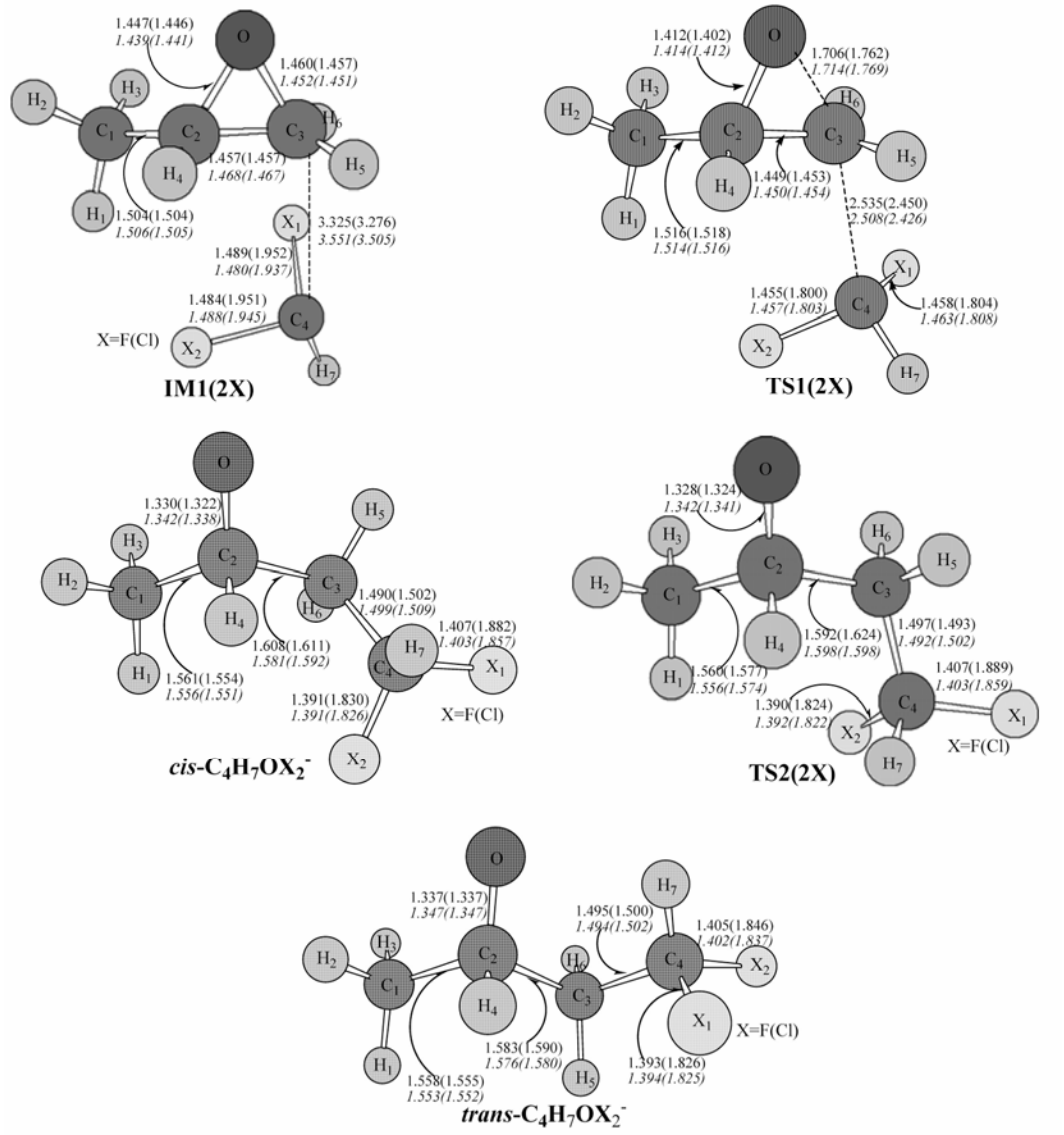

Figure 2. Optimized structures of the intermediate complexes (IM(2X)), transition states (TSn(2X)), and products (*cis*-$C_4H_7OX_2^-$ and *trans*-$C_4H_7OX_2^-$) along the B3LYP/6-311+G** reaction paths in the gas phase and in the Et_2O solvent. Values are the bond distances in Å. The values in italic are the bond distances in the Et_2O solvent and the values in parentheses are the bond distances when X denotes Cl.

cis-product anion and *trans*-product anion (see figures 1 and 2) for the two reactions, respectively, by the X (or X1) atom is in *cis*-conformation or *trans*-conformation to the O atom in this conformer. To the best of our knowledge, there is no reported theoretical study of these kinds of reactions.

In this work, the reactions (1) and (2) are computational studies using the DFT (density functional theory[17,18]) B3LYP [Becke's three-parameter hybrid functional[19] (B3) with the non-local correlation of Lee-Yang-Parr[20] (LYP)] method for the reaction path calculations in gas phase and the ether (Et_2O) solvent, including geometry optimization, frequency analysis, and IRC (intrinsic reaction coordinate)[21,22] calculations. The SCIPCM (self-consistent isodensity polarizable continuum) model[23] of the SCRF theory is used to simulate solution effects. We discuss here the accurate calculation results for the above model systems, which should be useful for experiment.

2. Computations

Atom labellings used for the reaction system are shown in figures 1 and 2. The nucleophilic halogenalkylation mechanisms of propylene oxide with CH_2X^- and CHX_2^- (X = F, Cl) in gas phase and the Et_2O solvent are studied at the B3LYP/6-311+G** level. Compared with the spherical cavity used in the Onsager model, the SCIPCM model uses the improved cavity defined by an isodensity surface coupled with the electron density of the solute molecule. As recommended by Wiberg and Rablen,[24] we used an isodensity value of 0·0004 for the SCIPCM model. We only considered the solvent of Et_2O with dielectric constant value 4·335 as a model solvent in simulating the effect of solvent.

In the gas phase we performed B3LYP geometry optimization calculations for locating stationary points along the reaction paths and B3LYP frequency analysis calculations for characterizing stationary points as intermediates (IMn) or transition states (TSn) and evaluating zero-point energies (ZPEs), and we denote these calculations in the gas phase as gas-B3LYP calculations. For locating and characterizing stationary points along the reaction paths of the four reactions in the solvent, we performed B3LYP geometry optimization and frequency analysis calculations using the SCIPCM model, and we denote these calculations in the solvent as SCIPCM-B3LYP calculations. To check the reaction paths, we performed gas-B3LYP and SCIPCM-B3LYP IRC calculations starting at transition states. All the gas-B3LYP and SCIPCM-B3LYP calculations were carried out using Gaussian 03 program.[25]

3. Results and discussions

3.1 *Nucleophilic halogenalkylation of propylene oxide with CH_2X^- (X = F, Cl)*

3.1a *Nucleophilic fluoroalkylation of propylene oxide with CH_2F^-:* Our (gas-B3LYP and SCIPCM-B3LYP) calculations predict the same reaction path (the same mechanism) for nucleophilic fluoroalkylation of propylene oxide in gas phase and the Et_2O solvent. We have drawn the potential energy curve in figure 3a, along which there are two transition states (TS1(F) and TS2(F)) and one intermediate (IM1(F)). In figure 3a we have also given the gas-B3LYP and SCIPCM-B3LYP relative energies (to the $C_3H_6O + CH_2F^-$ reactant) with ZPE corrections of the reactant ($C_3H_6O + CH_2F^-$), intermediate complex (IM1(F)), transition states (TS1(F) and TS2(F)), and the products (*cis*-$C_4H_8OX^-$ and *trans*-$C_4H_8OX^-$) for reaction (1) in the gas phase and the Et_2O solvent. We use the relative energies to reactants ($C_3H_6O + CH_2F^-$) in discussions in sections 3·1 and 3·2 unless otherwise noted. The calculations predict similar geometries (except IM1(F)) for each of the stationary-point species in both the gas phase and the Et_2O solvent. The optimized structures of IM1(F), TS1(F), *cis*-$C_4H_8OF^-$, TS2(F), and *trans*-$C_4H_8OF^-$, together with partial bond distance values, are shown in figure 1.

The B3LYP calculations indicate that reaction involves formation of IM1(F) (C_3H_6O–CH_2F^-) followed by a decomposition process of C_3–O bond in IM1(F) via TS1(F) leading to the *cis*-product (*cis*-$C_4H_8OF^-$), and the *cis*-product then transforming to a more stable *trans*-product (*trans*-$C_4H_8OF^-$) via TS2(F). Therefore, reaction (1) is considered to have steps 1 and 2. In the decomposition process of IM1(F) (step 1), the C_3–O bond breaks and the C_3–C_4 bond forms. With the C_3–C_4 bond rotating along the C_2–C_3 bond, a conformational isomer of the product (*cis*-$C_4H_8OF^-$) transforms to another more stable isomer of the product (*trans*-$C_4H_8OF^-$) via TS2(F) (step 2).

In the structures of IM1(F) (C_3H_6O–CH_2F^-), the C_3–O bond distances 1·471 and 1·458 Å are significantly longer than the normal C_3–O single-bond lengths of 1·434 and 1·440 Å in the gas phase and in the Et_2O solvent, respectively (see figure 1). As shown in figure 3a, the relative energy of IM1(F) is 8·56 kcal mol^{-1} lower than the value of reactant in the gas phase, but in the Et_2O solvent the relative energy of IM1(F) is 1·32 kcal mol^{-1} higher than the value of reactant. The difference of relative energy can be attributed to the change of the structures in the two phases. For example, the C_3–O bond in IM1(F) is much longer in the gas phase than in the Et_2O solvent while the C_3–C_4 and C_4–F distance values are larger in the Et_2O solvent. The $C_1C_2C_3C_4$, $C_2C_3C_4F$, and $OC_2C_3C_4$ dihedral angle values in the gas phase are –91·3°, –120·3° and 163·6°, respectively, while the corresponding values are –121·9°, –85·3°, and 134·1° in the Et_2O solvent, respectively (see table 1).

The IRC calculations in gas phase and the Et_2O solvent indicate that TS1(F) is connected to IM1(F). The barrier heights for step 1 of reaction (1) (the

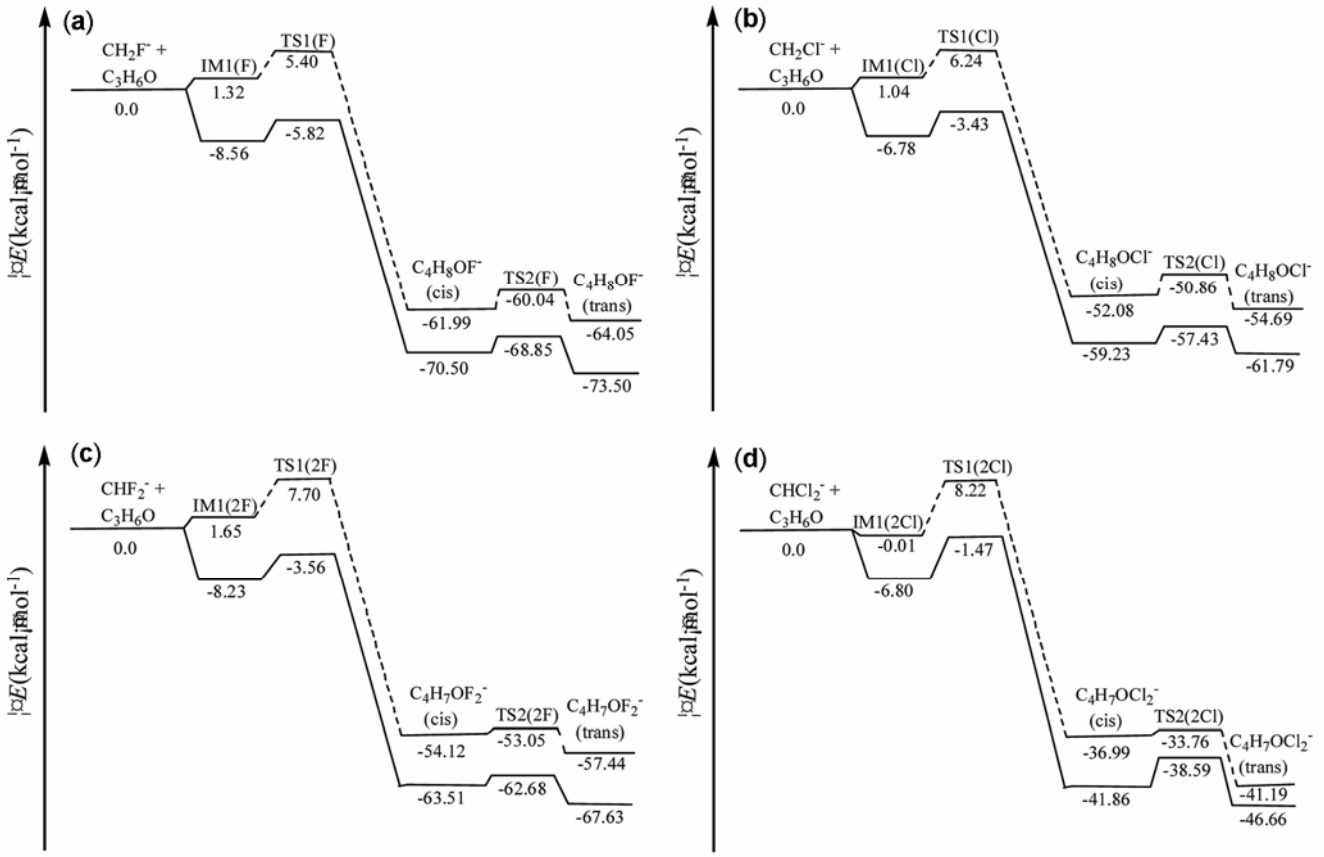

Figure 3. Schematic diagram of the potential energy curves along the reaction paths for the nucleophilic halogenalkylation of propylene oxide with CH_2X^- or CHX_2^- (X = F, Cl) in the gas phase (solid line) and in the Et_2O solvent (dashed line). (**a**) the nucleophilic fluoroalkylation of propylene oxide with CH_2F^-, (**b**) the nucleophilic chloroalkylation of propylene oxide with CH_2Cl^-, (**c**) the nucleophilic fluoroalkylation of propylene oxide with CHF_2^-, (**d**) the nucleophilic chloroalkylation of propylene oxide with $CHCl_2^-$. Values are the relative energies for the stationary-point species in the two phases.

relative energies of TS1(F) to IM1(F)) are predicted to be 2·74 and 4·08 kcal mol^{-1} in the gas phase and in the Et_2O solvent, respectively. Comparing with the values of TS1(F) in the gas phase, the C_4–F bond distance value increases and the C_3–C_4 bond distance value decreases in the Et_2O solvent.

The relative energies of *cis*-$C_4H_8OF^-$ are −70·50 and −61·99 kcal mol^{-1} in the gas phase and in the Et_2O solvent, respectively, which indicates that the *cis*-$C_4H_8OF^-$ is a stable product. In the structure of *cis*-$C_4H_8OF^-$, the C_3–O and C_2–C_3 bond distances are longer and the C_3–C_4 distance is shorter than the corresponding values in the structure of TS1(F) (figure 1). The O, C_2, C_3, and C_4 atoms in the structures of *cis*-$C_4H_8OF^-$ are almost co-planar (see the $OC_2C_3C_4$ dihedral angle values in table 1).

When the C_3–C_4 bond rotating along the C_2–C_3 bond, *cis*-$C_4H_8OF^-$ transforms to *trans*-$C_4H_8OF^-$ via TS2(F). The most obvious differences in the structures of *cis*-$C_4H_8OF^-$, TS2(F), and *trans*-$C_4H_8OF^-$ are the $C_1C_2C_3C_4$ and $OC_2C_3C_4$ dihedral angle values. For example, the $OC_2C_3C_4$ dihedral angle value in the structure of *cis*-$C_4H_8OF^-$ in the Et_2O solvent is almost 180·0° (176·6°) as mentioned above, while the corresponding values in the structures of TS2(F) and *trans*-$C_4H_8OF^-$ are 118·1° and 54·7°, respectively. The IRC calculations in both the gas phase and the Et_2O solvent indicate that TS2(F) is connected to *cis*-$C_4H_8OF^-$ in the back direction and to *trans*-$C_4H_8OF^-$ product of reaction (1) (X = F) in the forward direction. In the structure of *trans*-C_4H_8OF, as the major part of the product of reaction (1), the C_1, C_2, C_3, C_4 and F atoms are almost co-planar in both phases, and the F atom is in *trans*-conformation to the O atom.

The product of *trans*-$C_4H_8OF^-$ of reaction (1) (X = F) is predicted to be lower in energy than the reactant ($C_3H_6O + CH_2F^-$) by 73·50 and 64·50

Table 1. Gas-B3LYP/6-311+G** and SCIPCM-B3LYP/6-311+G** dihedral angles[a,b] of intermediate complex (IM1(X)), transition states (TS1(X) and TS2(X)), and products (*cis*-$C_4H_8OX^-$ (X = F, Cl) and *trans*-$C_4H_8OF^-$ (X = F, Cl)) in the gas phase and in the Et_2O solvent.

	$\angle C_1C_2C_3C_4$	$\angle C_2C_3C_4X$	$\angle OC_2C_3C_4$
IM1(F)	–91·3 (–121·9)[c]	–120·3 (–85·3)	163·6 (134·1)
TS1(F)	–75·9 (–76·1)	–135·8 (–126·4)	173·5 (173·2)
cis-$C_4H_8OF^-$	–57·5 (–58·7)	–168·5 (–169·9)	176·6 (175·4)
TS2(F)	–112·4 (–115·0)	–177·4 (–176·9)	120·8 (118·1)
trans-$C_4H_8OF^-$	179·4 (–178·9)	–178·6 (–177·8)	53·0 (54·7)
IM1(Cl)	–78·2 (–94·8)	–118·2 (–98·0)	176·7 (160·1)
TS1(Cl)	–68·6 (–69·8)	177·5 (–168·9)	180·0 (178·9)
cis-$C_4H_8OCl^-$	–57·9 (–59·6)	–172·1 (–173·0)	176·6 (174·8)
TS2(Cl)	–115·0 (–116·8)	–177·4 (–177·0)	118·4 (116·6)
trans-$C_4H_8OCl^-$	178·1 (–179·6)	–176·5 (–113·1)	51·8 (54·2)

[a]For labellings, see figure 2, where the B3LYP/6-311+G** bond lengths are given. [b]Dihedral angles are given in degrees. [c]Values in parentheses are the values of dihedral angles in the in the Et_2O solvent.

kcal mol^{-1} in gas phase and in the Et_2O solvent, respectively, which demonstrate reaction (1) (X = F) is exothermic in gas phase and the Et_2O solvent. The barrier heights for step 2 of reaction (1) (X = F) (the relative energies of TS2(F) to *cis*-$C_4H_8OF^-$) are predicted to be 1·65 and 1·95 kcal mol^{-1} in gas phase and in the Et_2O solvent, respectively. Since TS1(F) is obviously higher in energy than TS2(F) in both the two phases, the relative energies of TS1(F) to the IM1(F) are the overall barrier heights for reaction (1) (X = F). The overall barrier heights for reaction (1) (X = F) are predicted to be 2·74 and 4·08 kcal mol^{-1} in the gas phase and in the Et_2O solvent, respectively. Though there are little examples in the literature related to nucleophilic fluoroalkylation of simple epoxides, the low overall barrier heights for reaction (1) (X = F) predict CH_2F^- can react easily with propylene oxide kinetically.

3.1b *Nucleophilic chloroalkylation of propylene oxide with CH_2Cl^-:* Figure 3b shows the reaction path for the nucleophilic chloroalkylation of propylene oxide with CH_2Cl^- reaction in gas phase and the Et_2O, together with the gas-B3LYP and SCIPCM-B3LYP relative energies with ZPE corrections of respective species for reaction (1) (X = Cl) in gas phase and the Et_2O solvent. The calculations predict similar geometries (except IM1(Cl)) for each of the stationary-point species in gas phase and the Et_2O solvent. The optimized structures of IM1(Cl), TS1(Cl), *cis*-$C_4H_8OCl^-$, TS2(Cl), and *trans*-$C_4H_8OCl^-$ in both phases, together with partial bond distance values, are shown in parentheses of figure 1.

The reaction mechanisms for the nucleophilic chloroalkylation of propylene oxide with CH_2Cl^- and CH_2F^- are similar in gas phase and Et_2O solvent: $C_3H_6O + CH_2Cl^- \rightarrow$ IM1(Cl) (C_3H_6O–CH_2Cl^-) $\rightarrow$ TS1(Cl) $\rightarrow$ *cis*-$C_4H_8OCl^- \rightarrow$ TS2(Cl) $\rightarrow$ *trans*-$C_4H_8OCl^-$ (figure 3b).

The IRC calculations in gas phase and the Et_2O solvent indicate that TS1(Cl) is connected to IM1(Cl). The O, C_2, C_3, C_4, and Cl atoms in the structure of TS1(Cl) are almost co-planar in both phases (table 1). The relative energies of TS1(Cl) to IM1(Cl) are predicted to be 3·35 and 5·20 kcal mol^{-1} in the gas phase and in the Et_2O solvent, respectively. As shown in figure 1, the C_3–O bond distance in TS1(Cl) (1·702 Å) is longer than that (1·676 Å) in TS1(F) in the gas phase, while the C_3–C_4 distances are 2·539 and 2·613 Å in TS1(Cl) and TS1(F), respectively.

Comparing with the relative energies of *cis*-$C_4H_8OF^-$ (–70·50 and –61·99 kcal mol^{-1}), the relative energies of *cis*-$C_4H_8OCl^-$ of –59·23 and, –52·08 kcal mol^{-1} indicate the *cis*-$C_4H_8OCl^-$ is not as stable as *cis*-$C_4H_8OF^-$ thermodynamically in the two phases.

The structure of *cis*-$C_4H_8OCl^-$ transforms to *trans*-$C_4H_8OCl^-$ via TS2(Cl) with the C_3–C_4 bond rotating along the C_2–C_3 bond, which can be found by examining the $C_1C_2C_3C_4$ and $OC_2C_3C_4$ dihedral angle values (table 1). The IRC calculations indicate that TS2(Cl) is connected to *cis*-$C_4H_8OCl^-$ in the back direction and to *trans*-$C_4H_8OCl^-$ product of reaction (1) (X = Cl) in the forward direction.

The product of *trans*-$C_4H_8OCl^-$ of reaction (1) (X = Cl) is predicted to be lower in energy than the reactant ($C_3H_6O + CH_2Cl^-$) by 61·79 and 54·69 kcal mol^{-1} in gas phase and the Et_2O solvent, respectively, and reaction (1) (X = Cl) is exothermic and CH_2Cl^- can react easily with propylene oxide thermo-

Table 2. Gas-B3LYP/6-311+G** and SCIPCM-B3LYP/6-311+G** dihedral angles[a,b] of intermediate complex (IM1(2X)), transition states (TS1(2X) and TS2(2X)), and products (*cis*-$C_4H_7OX_2^-$ (X=F, Cl) and *trans*-$C_4H_7OF_2^-$ (X = F, Cl)) in the gas phase and in the Et_2O solvent.

	$\angle C_1C_2C_3C_4$	$\angle C_2C_3C_4X_1$	$\angle C_2C_3C_4X_2$	$\angle OC_2C_3C_4$
IM1(2F)	–51·7 (–3·0)[c]	98·1 (121·8)	–0·7 (16·9)	–157·8 (–107·8)
TS1(2F)	–63·3 (–64·0)	131·7 (129·0)	23·6 (20·6)	–175·2 (–175·7)
cis-$C_4H_7OF_2^-$	–63·0 (–63·3)	–155·4 (–159·2)	86·8 (83·7)	170·6 (170·5)
TS2(2F)	–109·2 (–113·1)	–168·7 (–170·5)	73·6 (72·5)	124·3 (120·5)
trans-$C_4H_7OF_2^-$	177·9 (178·9)	81·9 (77·9)	–161·3 (–165·4)	52·5 (53·3)
IM1(2Cl)	–62·9 (–4·8)	104·7 (25·0)	–2·0 (–83·9)	–168·6 (–109·4)
TS1(2Cl)	–64·7 (–65·0)	137·6 (136·2)	21·5 (18·8)	–178·0 (–178·0)
cis-$C_4H_7OCl_2^-$	–62·2 (–62·5)	–142·1 (–145·0)	94·3 (92·0)	171·6 (171·2)
TS2(2Cl)	–83·4 (–84·2)	–161·0 (–164·5)	75·4 (72·3)	151·0 (150·1)
trans-$C_4H_7OCl_2^-$	172·3 (174·2)	80·4 (78·0)	–156·9 (–159·3)	47·2 (48·9)

[a]For labellings, see figure 2, where the B3LYP/6-311+G** bond lengths are given. [b]Dihedral angles are given in degrees. [c]Values in parentheses are the values of dihedral angles in the in the Et_2O solvent.

dynamically in the two phases. The barrier heights for step 2 of reaction (1) (X = Cl) (the relative energies of TS2(Cl) to *cis*-$C_4H_8OCl^-$) are predicted to be 1·80 and 1·22 kcal mol^{-1} in gas phase and the Et_2O solvent, respectively. The relative energies of TS1(Cl) to the IM1(Cl) of 3·35 and 5·20 kcal mol^{-1} in the two phases are considered as the overall barrier heights for reaction (1) (X = Cl). The low overall barrier heights for reaction (1) (X = Cl) predict CH_2Cl^- can also react easily with propylene oxide kinetically as CH_2F^-. We conclude that propylene oxide can react more easily with CH_2F^- than with CH_2Cl^-, which can be estimated by the thermodynamic fact (the relative energies of *trans*-$C_4H_8OX^-$ to the reactant) and the kinetic fact (the overall barrier heights for reaction (1)). The relative energies of *trans*-$C_4H_8OCl^-$ to C_3H_6O + CH_2Cl^- are 11·71 and 9·36 kcal mol^{-1} higher than the corresponding values of *trans*-$C_4H_8OF^-$ to C_3H_6O + CH_2F^- in the gas phase and Et_2O solvent, respectively. The overall barrier heights of 3·35 and 5·20 kcal mol^{-1} for reaction (1) (X = Cl) are higher than the overall barrier heights of 2·74 and 4·08 kcal mol^{-1} for reaction (1) (X = F) in the gas phase and the Et_2O solvent, respectively.

3.2 *Nucleophilic halogenalkylation of propylene oxide with CHX_2^- (X = F, Cl)*

Figures 3c and d show the reaction path for the nucleophilic chloroalkylation of propylene oxide with CHX_2^- (X = F, Cl) reaction, respectively, in gas phase and the Et_2O solvent, together with the gas-B3LYP and SCIPCM-B3LYP relative energies (to the C_3H_6O + CHX_2^- reactant) with ZPE corrections of the reactant (C_3H_6O + CHX_2^-), intermediate complex (IM1(2X)), transition states (TS1(2X) and TS2(2X)), and the products (*cis*-$C_4H_7OX_2^-$ and *trans*-$C_4H_7OX_2^-$) for reaction (2) in both the gas phase and the Et_2O solvent. The B3LYP calculations predict similar geometries (except IM1(2X)) for each of the stationary-point species in both the gas phase and the Et_2O solvent. The optimized structures of IM1(2X), TS1(2X), *cis*-$C_4H_7OX_2^-$, TS2(2X), and *trans*-$C_4H_7OX_2^-$, together with partial bond distance values, are shown in figure 2.

Similar to the reaction path for the nucleophilic chloroalkylation of propylene oxide with CH_2X^-, the two reaction processes for the nucleophilic chloroalkylation of propylene oxide with CHX_2^- both consist of two reaction steps. The first step is the C_3–O bond breaking and the C_3–C_4 bond forming. The second step is the *cis*-product transforming to the *trans*-product with C_3–C_4 bond rotating along the C_2–C_3 bond. The reaction mechanisms are as follows: reactant (C_3H_6O + CHF_2^-) → IM1(2F) (C_3H_6O–CHF_2^-) → TS1(2F) → *cis*-$C_4H_7OF_2^-$ → TS2(2F) → *trans*-$C_4H_7OF_2^-$ (figure 3c), and reactant (C_3H_6O + $CHCl_2^-$) → IM1(2Cl) (C_3H_6O–$CHCl_2^-$) → TS1(2Cl) → *cis*-$C_4H_7OCl_2^-$ → TS2(2Cl) → *trans*-$C_4H_7OCl_2^-$ (figure 3(d)).

Along the reaction path for the nucleophilic chloroalkylation of propylene oxide with CHX_2^-,

IRC calculations in both the gas phase and the Et_2O solvent indicate that TS1(2X) is connected to IM1(2X), and TS2(2X) is connected to *cis*-$C_4H_7OX_2^-$ in the back direction and to *trans*-$C_4H_7OX_2^-$ product of reaction (2) in the forward direction.

The B3LYP calculations predict the same reaction path for reaction reactions (1) (X = F, Cl) and (2) (X = F) in the two phases, but there is a little difference about the relative energy of IM1(2Cl) in the gas phase and in the Et_2O solvent for reaction (2) (X = Cl).

We made a comparative study of the four reaction mechanisms. The relative energies of *trans*-$C_4H_8OF^-$, *trans*-$C_4H_8OCl^-$, *trans*-$C_4H_7OF_2^-$, and *trans*-$C_4H_7OCl_2^-$ to the respective reactants are predicted to be –73·05 and –64·50 kcal mol^{-1}, –61·79 and –54·69 kcal mol^{-1}, –67·63 and –57·44 kcal mol^{-1}, and –46·66 and –41·19 kcal mol^{-1} in the gas phase and in Et_2O solvent, respectively, which indicate that reactions (1) (X = F, Cl) and (2) (X = F, Cl) are exothermic and easy to react thermodynamically in both the gas phase and the Et_2O solvent. Therefore, their forward reactions have more advantage than their respective reverse reactions. The overall barrier energies for reactions (1) (X = F), reactions (1) (X = Cl), reactions (2) (X = F), and reactions (2) (X = Cl) are predicted to be 2·74 and 4·08 kcal mol^{-1}, 3·35 and 5·20 kcal mol^{-1}, 4·67 and 6·05 kcal mol^{-1}, and 5·33 and 8·23 kcal mol^{-1} in the gas phase and in the Et_2O solvent, respectively. Reaction (2) (X = Cl) has the highest barrier while reaction (1) (X = F) has the lowest barrier, so the kinetic order as the easy degree for the four reactions in both the phases are as follows: reaction (1) (X = F) > reaction (1) (X = Cl) > reaction (2) (X = F) > reaction (2) (X = Cl). The highest barrier in the four reactions are only 5·33 and 8·23 kcal mol^{-1} in gas phase and in the Et_2O solvent, therefore, we conclude that the nucleophilic halogenalkylation of propylene oxide with CH_2X^- or CHX_2^- (X = F, Cl) is relatively easy theoretically.

4. Conclusion

We studied reaction of the nucleophilic halogenalkylation of propylene oxide with CH_2X^- or CHX_2^- (X = F, Cl) producing *trans*-$C_4H_8OX^-$ or *trans*-$C_4H_7OX_2^-$ in the gas phase and in the Et_2O solvent, using the SCIPCM model of the SCRF theory for simulating solution effects and the B3LYP method for geometry optimization, frequency analysis, and IRC calculations.

Our calculations predict similar geometries (except IM1(X) and IM1 (2X)) for each of the stationary-point species in both the gas phase and the Et_2O solvent. Our calculations also predict the same reaction path for reactions (1) (X = F, Cl) and (2) (X = F) in the two phases, but there is a little difference about the relative energy of IM1(2Cl) in the gas phase and in the Et_2O solvent for reaction (2) (X = Cl). The four reaction processes consist of two reaction steps. The first step is the C_3–O bond breaking and the C_3–C_4 bond forming. The second step is the *cis*-product transforming to the *trans*-product with C_3–C_4 bond rotating along the C_2–C_3 bond. Reactions (1) and (2) are predicted to be exothermic and thermodynamically favourable in both the gas phase and the Et_2O solvent. TS1 is higher in energy than TS2 and the overall barrier energies for reactions (1) (X = F), reactions (1) (X = Cl), reactions (2) (X = F), and reactions (2) (X = Cl) are predicted to be 2·74 and 4·08 kcal mol^{-1}, 3·35 and 5·20 kcal mol^{-1}, 4·67 and 6·05 kcal mol^{-1}, and 5·33 and 8·23 kcal mol^{-1} in the gas phase and in the Et_2O solvent, respectively. We would expect that the accurate calculation of results for the model systems would be useful for the experimental researchers working in this field.

Acknowledgements

This work was supported by the China Postdoctoral Science Foundation Funded Project (No. 20080430193), Shandong Province Postdoctoral Innovation Foundation Funded Project China (No. 200702020), Natural Science Foundation Committee of Shandong Province (No. ZR2009BM003) to Dr. Zhang-Yu Yu, and the Education Department of Shandong Province (No. J09LB54), the Youth Fund of Jining University (2009QNKJ08) to Dr. Tao Liu.

References

1. Welch J T and Eswarakrishnan S 1991 *Fluorine in bioorganic chemistry* (New York: Wiley)
2. Kirsch P 2004 *Modern fluoroorganic chemistry* (Weinheim: Wiley-VCH)
3. Ni C, Li Y and Hu J 2006 *J. Org. Chem.* **71** 6829
4. Prakash G K S and Yudin A K 1997 *Chem. Rev.* **97** 757
5. Prakash G K S and Mandal M 2001 *J. Fluorine Chem.* **112** 123
6. Prakash G K S and Hu J 2005 *New nucleophilic fluoroalkylation chemistry.* In *Fluorine-containing synthons* (ed.) Soloshonok V A (Washington, DC: American Chemical Society)

7. Prakash G K S and Hu J 2005 *Trihalomethyl compounds.* In *Science of synthesis* (ed.) Charette A B (New York: Thieme)
8. Singh R P and Shreeve J M 2000 *Tetrahedron* **56** 7613
9. Langlois B R and Billard T 2003 *Synthesis* **2003** 185
10. Ait-Mohand S, Takechi N, Medebielle M and Dolbier W R Jr 2001 *Org. Lett.* **3** 4271
11. McClinton M A and McClinton D A 1992 *Tetrahedron* **48** 6555
12. Burton D J and Yang Z Y 1992 *Tetrahedron* **48** 189
13. Ni C and Hu J 2005 *Tetrahedron Lett.* **46** 8273
14. Li Y and Hu J 2005 *Angew. Chem., Int. Ed.* **44** 5882
15. Li Y, Ni C, Liu J, Zhang L, Zheng J, Zhu L and Hu J 2006 *Org. Lett.* **8** 1693
16. Takechi N, Ait-Mohand S, Medebielle M and Dolbier W R Jr 2002 *Org. Lett.* **4** 4671
17. Hohenberg P and Kohn W 1964 *Phys. Rev. B: Condens. Matter* **136** 864
18. Kohn W and Sham L 1965 *J. Phys. Rev. A: At. Mol. Opt. Phys.* **140** 1133
19. Becke A D 1993 *J. Chem. Phys.* **98** 5648
20. Lee C, Yang W and Parr R G 1988 *Phys. Rev. B: Condens. Matter.* **37** 785
21. Gonzalez C and Schlegel H B 1989 *J. Chem. Phys.* **90** 2154
22. Gonzalez C and Schlegel H B 1990 *J. Phys. Chem.* **94** 5523
23. Foresman J B, Keith T A, Wiberg K B, Snoonian J and Frisch M J 1996 *J. Phys. Chem.* **100** 16098
24. Wiberg K B and Rablen P R 1993 *J. Comput. Chem.* **14** 1504
25. Frisch M J *et al* 2003 Gaussian 03W, Gaussian, Inc., Pittsburgh, PA